Gas-phase reactions of anions with halogenated methanes at 297 ± 2 K

K. TANAKA, G. I. MACKAY, J. D. PAYZANT,[1] AND D. K. BOHME[2]

Department of Chemistry, York University, Downsview, Ontario M3J 1P3

Received September 23, 1975

K. TANAKA, G. I. MACKAY, J. D. PAYZANT, and D. K. BOHME. Can. J. Chem. **54**, 1643 (1976).

The rate constants for a number of exothermic displacement (S_N2) reactions of the type $X^- + CH_3Y \rightarrow Y^- + CH_3X$ where $X^- = H^-$, O^-, C^-, F^-, S^-, Cl^-, OH^-, C_2^-, CN^-, SH^-, S_2^-, C_2H^-, NH_2^-, NO_2^-, CHF^-, CH_2Cl^-, CH_2Br^-, CH_3O^-, CH_3S^-, and CH_3NH^- and Y = F, Cl, and Br, have been measured in the gas phase at 297 ± 2 K using the flowing afterglow technique. These gas-phase measurements provided an opportunity to determine the intrinsic nucleophilic reactivity of 'nude' anions and hence to assess the role of solvation in the kinetics of S_N2 reactions proceeding in solution. Comparisons of the experimental rate constants with rate constants calculated using classical theories of capture indicate that several displacement reactions may possess large *intrinsic* energies of activation, $E_a \gg 2$ kcal mol^{-1}. Correlations were found between apparent activation energies and the heats of reaction. These correlations provided a convenient classification of the various anion nucleophiles. Displacement was observed to compete with proton transfer in reactions involving nucleophiles of high intrinsic basicity and with hydrogen atom transfer and H_2^+ transfer in the reactions of the O^- radical anion.

K. TANAKA, G. I. MACKAY, J. D. PAYZANT et D. K. BOHME. Can. J. Chem. **54**, 1643 (1976).

Utilisant la technique de la lueur d'écoulement on a mesuré, en phase gaseuse, à 297 ± 2 K, les constantes de vitesse d'un certain nombre de réactions de déplacements exothermiques (S_N2) du type $X^- + CH_3Y \rightarrow Y^- + CH_3X$ ou $X^- = H^-$, O^-, C^-, F^-, S^-, Cl^-, OH^-, C_2^-, CN^-, SH^-, S_2^-, C_2H^-, NH_2^-, NO_2^-, CHF^-, CH_2Cl^-, CH_2Br^-, CH_3O^-, CH_3S^- et CH_3NH^- et Y = F, Cl et Br. Ces mesures en phase gaseuse fournissent une occasion de déterminer la réactivité nucléophile intrinsèque d'anions 'nus' et ainsi de déterminer le rôle de la solvatation dans la cinétique des réactions S_N2 se produisant en solution. Une comparaison des constantes de vitesse expérimentales avec les vitesses de réaction calculées en utilisant les théories classiques de capture indiquent que plusieurs réactions de déplacement peuvent posséder de grandes énergies intrinsèques d'activation, $E_a \gg 2$ kcal mol^{-1}. On a trouvé des corrélations entre les énergies d'activation apparentes et les chaleurs de réaction. Ces corrélations fournissent une classification commode des divers anions nucléophiles. On a observé que le déplacement est en compétition avec le transfert de protons dans la réaction impliquant des nucléophiles de basicités intrinsèques élevées et avec le transfert d'atome d'hydrogène et le transfert de H_2^+ dans les réactions de l'anion radical O^-.

[Traduit par le journal]

Introduction

The kinetics of nucleophilic displacement (S_N2) or CH_3^+ transfer reactions of the type

[1] $$X^- + CH_3Y \rightarrow Y^- + CH_3X$$

have been studied extensively in solution in a variety of protic and dipolar aprotic solvents (I). The second-order rate constants for these reactions measured at 25 °C have values generally $< 10^3$ l mol^{-1} s^{-1} ($< 10^{-18}$ cm^3 molecule^{-1} s^{-1}) and are extremely sensitive to the nature of the solvent, being often as much as 10^6 times faster in dipolar aprotic than in protic solvents. The reactions are characterized in solution by activation energies approximately in the range 15–30 kcal mol^{-1}. In order to attain an appreciation of the extent to which solvent determines the kinetics and energetics of such reactions in solution, Moelwyn-Hughes and co-workers (2) were the first to consider the intrinsic interactions between 'nude' ions, X^-, and polar molecules, CH_3Y. They were led to speculate that the solvent was entirely responsible for impeding these reactions in solution and to suppose that such reactions should proceed in the gas phase essentially in the absence of activation energies and with intrinsic rates which would be immeasurably fast. Gas-phase techniques have now become available which in fact allow the measurement of these intrinsic rates (3–5). Early, such measurements indicated

[1]Present address: Department of Chemistry, University of Alberta, Edmonton, Alberta.

[2]Alfred P. Sloan Research Fellow, 1974–1976.

that reactions of type [1] involving charge-localized anions could indeed proceed extremely rapidly in the gas phase and that solvation of the anion by one or more solvent molecules did in fact act to reduce the specific rate (3). These results prompted Won and Willi to reopen the discussion of the mechanism of the S_N2 reactions of methyl halides with nucleophiles in solution (6). Later measurements (5, 7) revealed several slow S_N2 reactions and suggested that energy barriers rather than orientation or steric effects were the important rate controlling factors as had been predicted in several molecular orbital calculations (8, 9).

In this paper we report a systematic study of exothermic reactions of type [1] between a variety of anions and the methyl halides CH_3F, CH_3Cl, and CH_3Br at 297 ± 2 K. The study was initiated in part to provide a characterization of the intrinsic behaviour of such reactions so that a comparison of this behaviour with that observed in solution would provide some appreciation of the extent to which the solvent dominates the kinetics and energetics of these reactions in solution.

Experimental

All experiments were performed using a flowing afterglow apparatus whose details of construction and operation have been described previously together with the concomitant data analysis (10). Helium was used as the carrier gas at flows in the range 0.9–2.1 × 10^{16} molecule s^{-1} with resulting average values of the total gas pressure in the range 0.256–0.592 torr. The anions were produced in a flowing plasma of helium containing a suitable parent gas. The plasma was generated with an electron gun operating at a filament emission of 1.0 mA with electron energies in the range 35–70 eV. The anions generated for this study and their parent gases were: H^- (NH_3, CH_4), NH_2^- (NH_3), OH^- (H_2O), CN^- (CH_3NH_2), CH_3O^- (CH_3OH), S^- (H_2S), SH^- (CH_3SH, H_2S), S_2^- (CH_3SH, H_2S), CH_3S^- (CH_3SH), CH_3NH^- (CH_3NH_2), C^- (C_2H_2), C_2^- (C_2H_2), C_2H^- (C_2H_2), O^- (H_2O, air), NO_2^- (air), Cl^- (CCl_4) and F^- (CF_4, CH_3F). The halogenated methanes were introduced sufficiently downstream of the anion production region to ensure that the anions had undergone a sufficient number of collisions (≫ 100) with the helium carrier gas to become thermalized at the ambient room temperature (297 ± 2 K). The effective reaction lengths were in the ranges 59–61 cm and 84–85 cm. The average gas velocity in the reaction region had values in the range 7.8–9.7 × 10^3 cm s^{-1}. Reaction rate constants were determined in the usual manner from measurements of changes in the anion signals as a function of the addition of the halogenated methane into the flowing plasma.

The gases used were He (Linde, Prepurified Grade, 99.995% He), NH_3 (Matheson, anhydrous, ≥99.99% NH_3 (liquid phase)), CH_4 (Matheson, Ultrahigh Purity, ≥99.97% CH_4), H_2O (boiled tap water), CH_3NH_2 (Matheson, ≥98.0% CH_3NH_2 (liquid phase)), CH_3OH (BDH Chemicals), H_2S (Matheson, C.P. Grade, ≥99.5% H_2S (liquid phase)), CH_3SH (Matheson, ≥99.5% CH_3SH (liquid phase)), C_2H_2 (Matheson, Purified, ≥99.6% C_2H_2), CCl_4 (BDH Chemicals), CF_4 (Matheson, ≥99.7% CF_4), CH_3F (Matheson, ≥99.0% CH_3F (liquid phase)), CH_3Cl (Matheson, ≥99.5% CH_3Cl (liquid phase)), and CH_3Br (Matheson, ≥99.5% CH_3Br (liquid phase)).

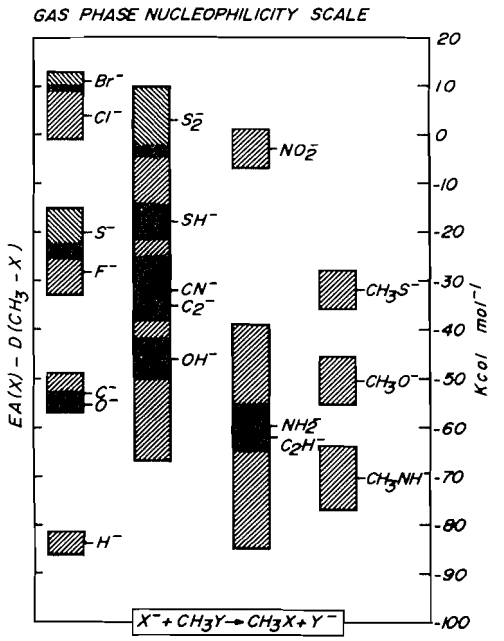

FIG. 1. Scale of thermodynamic nucleophilicity of anions in the gas phase. The width of the shaded areas represents the uncertainty.

Results

Sufficient thermodynamic information is now available to characterize the intrinsic thermodynamic nucleophilicity of many atomic, diatomic, and polyatomic anions in gas-phase reactions of type [I]. For these reactions the intrinsic thermodynamic nucleophilicity is determined by the electron affinity, EA(X), of the nucleophile and the H_3C—X bond strength of the neutral product since the overall standard enthalpy change may be expressed as

$$[2]\quad \Delta H^0 = \mathrm{EA(X)} - D^0(\mathrm{CH_3—X}) - \mathrm{EA(Y)} + D^0(\mathrm{CH_3—Y})$$

Figure 1 provides a scale of the thermodynamic nucleophilicity in the gas phase of most of the anions whose reactions were investigated in this

TABLE 1. Thermochemical information (in kcal mol^{-1}) employed in the characterization of the intrinsic thermodynamic nucleophilicity of anions in reactions of the type $X^- + CH_3Y \rightarrow Y^- + CH_3X$

X^-	$\Delta H^0_{f,298}(X)$	$EA^0_{298}(X)^a$	$\Delta H^0_{f,298}(X^-)^b$	$D^0_{298}(CH_3—X)^c$	$\Delta H^0_{f,298}(CH_3X)$	$EA^0_{298}(X) - D^0_{298}(CH_3—X)$
H^-	52.100±0.001 (11)	18.9±0.5	33.2±0.5 (11)	102.7±2.0 (12)	−17.90±0.08 (11)	−83.8±2.5
O^-	59.56±0.03 (11)	35.3±0.5	24.3±0.5 (11)	90.5±1.5	3.9±1.0 (13)	−55.2±2.0
C^-	170.89±0.45 (11)	30.4±0.4	140.5±0.8 (11)	83±3	123±3[d]	−53±4
F^-	18.86±0.40 (11)	79.94±0.05	−61.08±0.45 (14)	108±5 (12)	−56±7 (11)	−28±5
S^-	66.29±0.01 (14)	49.4±0.1 (15)	16.9±0.5	69±5 (12)	32.3 (16)	−20±5
Cl^-	28.989±0.02 (14)	84.9±0.5	−55.9±0.5 (11)	81±5 (12)	−20.0±0.5 (14)	4±6
Br^-	26.741 (16)	79.1±0.1 (17)	−52.3±0.5	68±2 (12)	−8.4 (16)	11±2
OH^-	9.492±0.040 (14)	43.81±0.9	−34.32±0.90 (14)	90±3 (12)	−47.96 (16)	−46±4
C_2-	200.2±0.9 (11)	94±20	106±20 (11)	127±12	108±11[e]	−33±32
CN^-	104.0±2.5 (11)	89.5±0.5	14.5±3 (14)	121±5[f] (12)	20.9[f] (16)	−32±6
SH^-	33.4±0.9 (18)	55.0±0.2 (19)	−21.0±1.1	73±3 (12)	−5.34 (16)	−18±3
S_2^-	30.84±0.20 (11)	39.9±0.9 (20)	−9.1±1.1	37±6	29±5[g]	3±7
C_2H^-	118±11 (11, 21)	47±12	71.5±1.1 (22)	109±11	44.32 (16)	−62±23
NH_2^-	44.9±1.7[h]	19.5±0.8 (20)	25.4±0.9 (23)	79±3 (12)	−5.49 (16)	−60±4
NO_2^-	7.91±0.2 (11)	56.4±1.2	−48.45±1.4 (14)	59±3[i] (12)	−17.86[i] (16)	−3±4
CH_3NH^-	43.6±2.0 (24)	13.1±3.5	30.5±1.5 (25)	83.6±3 (26)	−4.41± (16)	−70.5±6.5
CH_3O^-	3.9±1.0 (13)	30.9±2.3	−27.0±1.3[j]	81.4±3 (26)	−43.99 (16)	−50.5±5.3
CH_3S^-	32.3 (16)	44±1	−12±1[j]	76±3	−8.90 (16)	−32±4

[a] $EA^0_{298}(X)$ is calculated from $\Delta H^0_{f,298}(X)$ and $\Delta H^0_{f,298}(X^-)$ unless otherwise indicated.
[b] $\Delta H^0_{f,298}(X^-)$ is calculated from $\Delta H^0_{f,298}(X)$ and $EA^0_{298}(X)$ unless otherwise indicated.
[c] $D^0_{298}(CH_3—X)$ is calculated from the heats of formation of X, CH_3X, and CH_3 (11) unless otherwise indicated.
[d] Calculated from $C_2H_6 \rightarrow CH_3C + 3H$ using a total bond dissociation energy for the three C—H bonds of 300±3 kcal mol^{-1}.
[e] Calculated from $CH_3C_2H \rightarrow CH_3C_2 + H$ assuming that $D^0_{298}(CH_3C_2—H) \simeq D^0_{298}(HC_2—H) = 116 \pm 11$ kcal mol^{-1} determined from the heats of formation of HC_2, H, and C_2H_2 (11).
[f] $CH_3—CN$.
[g] Calculated from $CH_3S_2CH_3 \rightarrow CH_3S_2 + CH_3$ assuming that $D^0_{298}(CH_3S_2—CH_3) \simeq D^0_{298}(S—CH_3)$.
[h] Calculated from $\Delta H^0_{f,298}(NH_2^-)$ and $EA^0_{298}(NH_2)$.
[i] $CH_3—NO_2$.
[j] Unpublished results from this laboratory.

TABLE 2. Measured reaction and calculated capture rate constants (in units of 10^{-9} cm^3 molecule^{-1} s^{-1}) for exothermic reactions of anions with CH_3F in the gas phase at 297 ± 2 K

Anion	N^a	$k_{expt}{}^b$	$k_c{}^c$	$k_{expt}/k_c{}^d$	$-\Delta H^0_{298}$/(kcal mol^{-1})
H^-	4	0.015±0.002	7.6	0.0020±0.0004	56±8
O^-	3	1.1±0.1	2.3	0.48±0.09	27±7
C^-	3	⩽0.002	2.5	⩽0.0008	25±9
OH^-	5	0.025±0.002	2.2	0.011±0.003	18±9
C_2^-	3	⩽0.002	2.0	⩽0.001	5±37
CN^-	4	⩽0.003	1.9	⩽0.002	4±11[e]
C_2H^-	3	⩽0.0003	2.0	⩽0.0002	34±28[f]
NH_2^-	3	0.0176±0.0006	2.3	0.0076±0.0015	32±9
CHF^-	1	⩾0.41	1.8	⩾0.23	
CH_3O^-	3	0.014±0.002	1.9	0.0074±0.0016	23±10
CH_3S^-	1	⩽0.001	1.7	⩽0.0006	4±9
CH_3NH^-	1	0.05	1.9	0.03	43±12

[a] N is the number of measurements.
[b] The limits given along with the mean value of the measurements represent the best estimate of the precision (27). The accuracy is estimated to be ±20%.
[c] The capture rate constant is calculated using the Average-Dipole-Orientation Theory (28) with C = 0.23.
[d] The uncertainty in k_{expt}/k_c reflects only the accuracy of k_{expt}.
[e] For the formation of CH_3—CN.
[f] For the formation of CH_3—C≡CH.

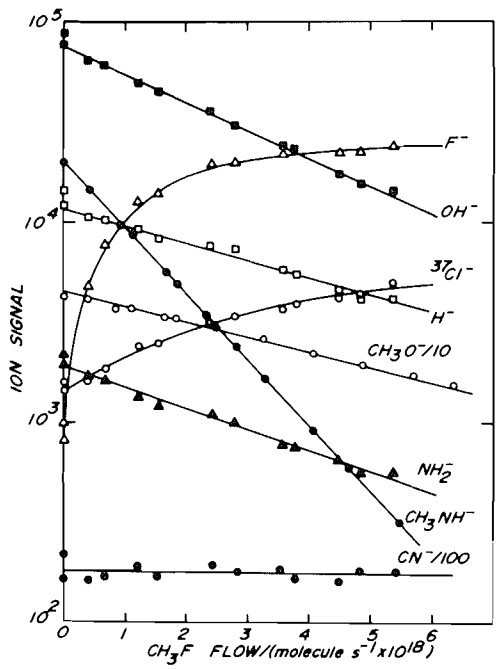

FIG. 2. Summary plot of the variation of anion signals observed as a function of CH_3F flow. T = 297 K, p = 0.331 torr, $\bar{v}$ = 8.1 × 10^3 cm s^{-1}, L = 84 cm, and the flow of NH_3 = 1.4 × 10^{17} molecule s^{-1} (H^-, NH_2^-, OH^-, and CN^-), of CH_3OH ~ 2 × 10^{17} molecule s^{-1} (CH_3O^-), and of CH_3NH_2 = 3.8 × 10^{18} molecule s^{-1} (CH_3NH^-).

study. Table 1 summarizes the thermodynamic information used to calculate these nucleophilicities. H^- is the 'strongest' nucleophile in Fig. 1 in the sense that the displacement of any nucleophile above it on this scale represents the thermodynamically preferred (exothermic) direction of displacement. The experiments reported here were intended to determine the specific rates at 297 ± 2 K for all the exothermic displacements of F^-, Cl^-, and Br^- from CH_3F, CH_3Cl, and CH_3Br respectively, which can be identified in Fig. 1. The measurement of the specific rates was always accompanied by a careful search for product ions since in several instances the displacement reaction was observed to compete with other reaction channels.

Summaries of the rate constant measurements are included in Tables 2, 3, and 4. Sources of error have been described previously (10). The absolute accuracy of the reported rate constants is estimated to be ±20%. A number of the measurements included in Tables 2 and 3 have been reported previously (7).

$X^- + CH_3F$

Figure 2 is representative of the observations of the exothermic displacement reactions of H^-, OH^-, NH_2^-, CH_3O^-, and CH_3NH^- with CH_3F for which the rate constants proved to be measurable. F^- was the only observed product ion in each case. The appearance of the Cl^- ion can be attributed to a chloride impurity (probably CH_3Cl) in CH_3F. The reactions were generally slow, having rate constants in the range 1–6 × 10^{-11} cm^3 molecule^{-1} s^{-1}.

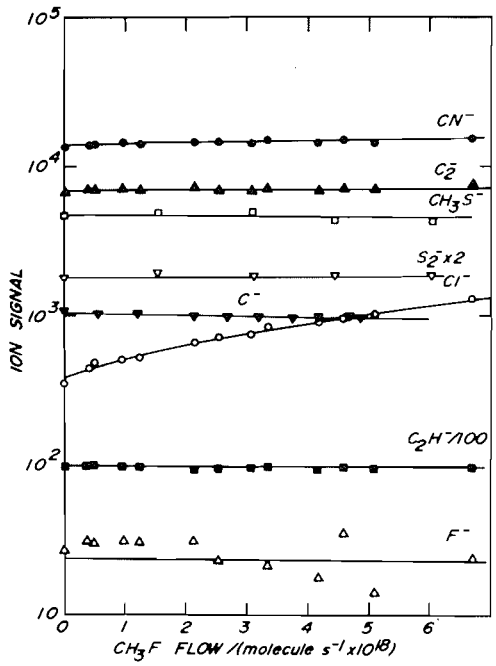

FIG. 3. The variation of anion signals observed as a function of CH_3F flow. $T = 295$ K, $p = 0.411$ torr, $\bar{v} = 8.7 \times 10^3$ cm s^{-1}, $L = 85$ cm, and the flow of $C_2H_2 = 1.5 \times 10^{18}$ molecule s^{-1}. The data of S_2^- and CH_3S^- are taken from another experiment. $T = 297$ K, $p = 0.360$ torr, $\bar{v} = 8.2 \times 10^3$ cm s^{-1}, $L = 85$ cm, and the flow of $CH_3SH = 7.1 \times 10^{17}$ molecule s^{-1}.

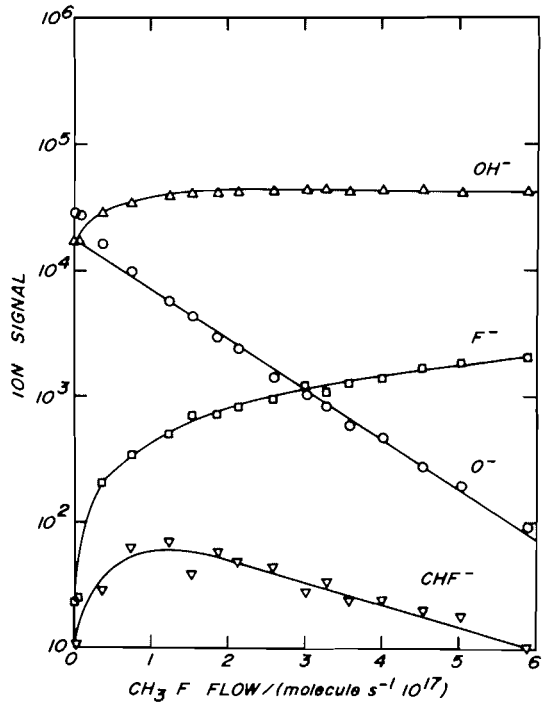

FIG. 4. The variation of the major ion signals observed for the reaction of O^- with CH_3F. $T = 295$ K, $p = 0.409$ torr, $\bar{v} = 8.3 \times 10^3$ cm s^{-1}, $L = 60$ cm, and the flow of $H_2O \sim 2 \times 10^{17}$ molecule s^{-1}.

Figure 3 includes observations of the exothermic reactions of anions with CH_3F with rate constants for which only an upper limit could be determined. Neither the C^-, CN^-, C_2^-, S_2^-, C_2H^-, and CH_3S^- signals nor the F^- signal, whose representative behaviour is included in Fig. 3, were observed to change upon the addition of CH_3F into flowing plasmas containing these ions. The increase in the Cl^- signal again reflects the presence of a chloride impurity in CH_3F.

Figure 4 shows the behaviour of the product ions observed upon the addition of CH_3F into a flowing H_2O–He plasma containing measurable amounts of O^- ions. O^- appears to react with CH_3F in three ways according to

$$[3a] \quad O^- + CH_3F \rightarrow OH^- + CH_2F$$

$$[3b] \quad \rightarrow F^- + CH_3O$$

$$[3c] \quad \rightarrow CHF^- + H_2O$$

Channel 3*a* corresponds to H-atom transfer and channel 3*c* to H_2^+ transfer. The CHF^- ion rapidly reacts further, apparently to produce F^- according to the displacement reaction 4

$$[4] \quad CHF^- + CH_3F \rightarrow F^- + (C_2H_4F)$$

Uncertainties (of at most a factor of three) associated with sampling and detection sensitivities and the further reactions of CHF^- and OH^- with CH_3F precluded a direct determination of the exact branching ratio for reaction 3. However, the H-atom transfer reaction is clearly the dominant channel. A fit to the OH^-, F^-, and CHF^- behaviour which ignored differences in sampling and detection sensitivities provided a branching ratio of approximately 98:1:1 for $OH^-:F^-:CHF^-$.

$X^- + CH_3Cl$

Figure 5 displays typical results observed for the reactions of H^-, F^-, OH^-, CH_3O^-, CN^-, and NO_2^- with CH_3Cl. H^-, F^-, and OH^- are seen to react rapidly to produce Cl^- whereas CN^- and NO_2^- do not react with a measurable rate in spite of the fact that these latter two

TABLE 3. Measured reaction and calculated capture rate constants (in units of 10^{-9} cm^3 molecule^{-1} s^{-1}) for exothermic reactions of anions with CH_3Cl in the gas phase at 297 ± 2 K

Anions	N^a	k_{expt} This work[b]	k_{expt} Other values	k_c[c]	k_{expt}/k_c[d]	$-\Delta H^0_{298}$/(kcal mol^{-1})
H^-	2	3.0±0.2	2.5 (4)	8.6	0.35±0.07	88±9
O^-	5	1.7±0.3	2.4 (3)	2.4	0.71±0.14	59±8
C^-	3	0.30±0.04		2.7	0.11±0.02	57±10
F^-	1	1.9	1.8 (4), 0.80±0.09 (5)	2.3	0.83±0.16	32±11
S^-	1	0.030		1.9	0.016±0.003	24±11
OH^-	4	1.5±0.1	1.9 (4)	2.4	0.62±0.13	50±10
C_2^-	3	⩽0.005		2.1	⩽0.002	37±38
CN^-	4	⩽0.0004		2.1	⩽0.0002	36±12[e]
SH^-	6	0.017±0.001		1.9	0.0089±0.0018	22±9
S_2^-	4	⩽0.001		1.6	⩽0.0006	1±13
C_2H^-	4	0.13±0.01	1.2 (7)[f]	2.1	0.062±0.014	66±29[g]
NH_2^-	3	1.5±0.2	2.1 (4)	2.4	0.63±0.13	64±10
NO_2^-	1	⩽0.0010		1.7	⩽0.00059	7±10[h]
CH_2Cl^-	4	0.51±0.04		1.7	0.30±0.06	
CH_3O^-	3	1.3±0.1	1.6 (4)	1.9	0.68±0.14	55±11
CH_3S^-	4	0.11±0.01	0.078±0.012 (5)	1.7	0.065±0.012	36±10
CH_3NH^-	3	1.7±0.1		2.0	0.85±0.17	75±13

[a] N is the number of measurements.
[b] The limits given along with the mean value of the measurements represent the best estimate of the precision (27). The accuracy is estimated to be ±20%.
[c] The capture rate constant is calculated using the Average-Dipole-Orientation Theory (28) with $C = 0.21$.
[d] The uncertainty in k_{expt}/k_c reflects only the accuracy of k_{expt}.
[e] For the formation of CH_3—CN.
[f] The previously reported high value (7) is in error. The origin of this error has been traced to a floating decimal in the data printout. k_{expt} should have been 0.12×10^{-9} cm^3 molecule^{-1} s^{-1}.
[g] For the formation of CH_3—C≡CH.
[h] For the formation of CH_3—NO_2.

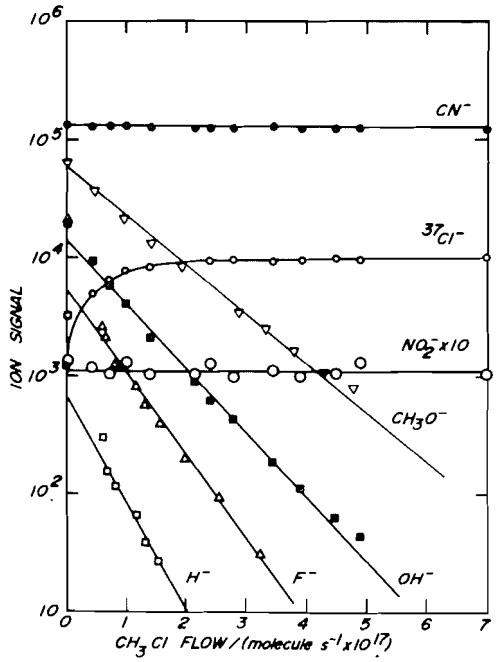

FIG. 5. The variation of anion signals observed as a function of CH_3Cl flow. T = 297 K, p = 0.289 torr, $\bar{v}$ = 8.3 × 10^3 cm s^{-1}, L = 59 cm, and the flow of CH_3F = 1.1 × 10^{17} molecule s^{-1}. H^-, OH^-, NO_2^-, and CN^- are present as impurity ions in this particular experiment. The CH_3O^- decay was taken from another experiment: T = 296 K, p = 0.332 torr, $\bar{v}$ = 8.9 × 10^3 cm s^{-1}, L = 59 cm, and the flow of CH_3OH ~ 4 × 10^{17} molecule s^{-1}.

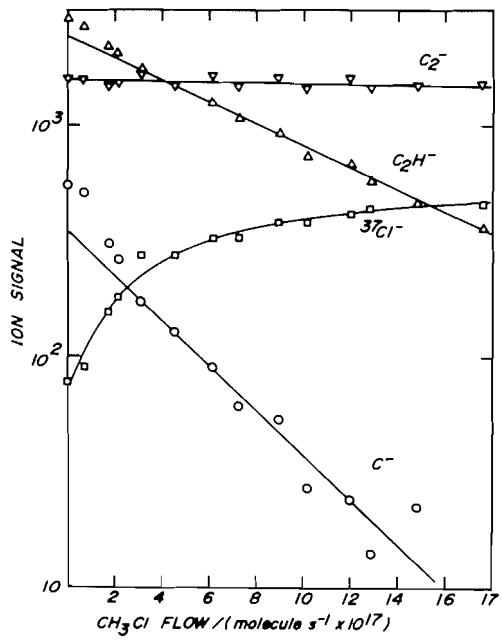

FIG. 6. The variation of carbonaceous anion signals observed as a function of CH_3Cl flow. T = 298 K, p = 0.433 torr, $\bar{v}$ = 8.3 × 10^3 cm s^{-1}, L = 60 cm, and the flow of C_2H_2 = 3.9 × 10^{17} molecule s^{-1}.

reactions are also exothermic. The results obtained for the reactions of the carbonaceous anions C^-, C_2^-, and C_2H^- and the sulfur containing anions S^-, SH^-, S_2^-, and CH_3S^- are shown in Figs. 6 and 7 respectively. A large range in the values of the rate constants for these reactions is again apparent.

Figures 8 and 9 include observations of the reactions of NH_2^- and CH_3NH^-, the two strongest bases of the anions investigated in this study, with CH_3Cl. Since independent experiments indicated that the reactions of OH^- and H^- with CH_3Cl proceed solely by Cl^- displacement, the observed production of CH_2Cl^- in Figs. 8 and 9 can be attributed to the proton transfer reactions

$$[5] \quad NH_2^- + CH_3Cl \rightarrow CH_2Cl^- + NH_3$$

$$[6] \quad CH_3NH^- + CH_3Cl \rightarrow CH_2Cl^- + CH_3NH_2$$

Again only a qualitative assessment could be made of the branching ratio, in this case the extent to which proton transfer competes with Cl^- displacement. Displacement does appear to be the predominant channel with *ca.* 10% of the collisions leading to proton transfer.

CH_2Cl^- is observed to react further with CH_3Cl according to

$$[7] \quad CH_2Cl^- + CH_3Cl \rightarrow Cl^- + (C_2H_5Cl)$$

Figure 10 displays the observation of the reactions of O^- with CH_3Cl

$$[8a] \quad O^- + CH_3Cl \rightarrow Cl^- + CH_3O$$

$$[8b] \quad \rightarrow OH^- + CH_2Cl$$

$$[8c] \quad \rightarrow CHCl^- + H_2O$$

The three channels are analogous to those observed for the reaction of O^- with CH_3F. H-atom transfer is, however, much less dominant with the displacement channel gaining in importance.

$X^- + CH_3Br$

Figures 11–13 are representative of the observations of the exothermic reactions of H^-, C^-, F^-, Cl^-, OH^-, C_2^-, CN^-, SH^-, S_2^-, C_2H^-, NO_2^-, CH_3O^-, and CH_3S^- with CH_3Br for

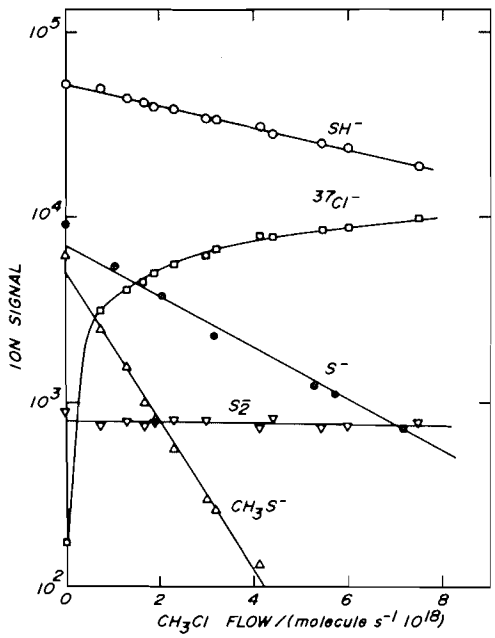

FIG. 7. The variation of sulfur containing anion signals as a function of CH_3Cl flow. T = 296 K, p = 0.347 torr, $\bar{v}$ = 8.5 × 10^3 cm s^{-1}, L = 59 cm, and the flow of CH_3SH = 7.4 × 10^{17} molecule s^{-1}. The data of S^- are taken from another experiment, T = 297 K, p = 0.336 torr, $\bar{v}$ = 8.4 × 10^3 cm, L = 85 cm, and the flow of CH_3SH = 1.5 × 10^{17} molecule s^{-1}.

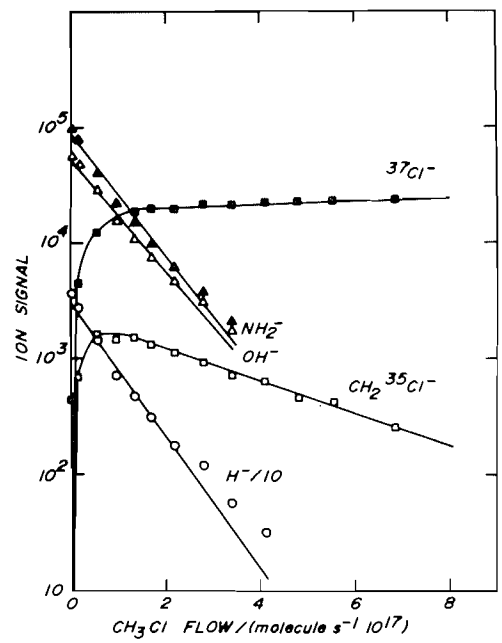

FIG. 8. The variation of the major ion signals observed for the reaction of NH_2^- with CH_3Cl. T = 296 K, p = 0.524 torr, $\bar{v}$ = 9.5 × 10^3 cm s^{-1}, L = 60 cm, and the flow of NH_3 = 4.3 × 10^{18} molecule s^{-1}.

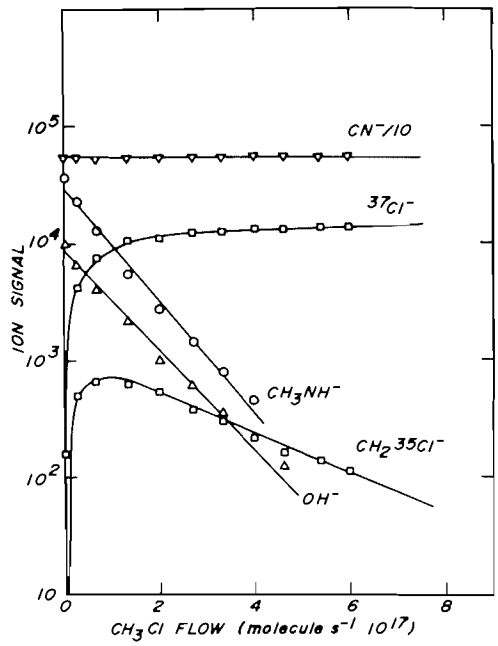

FIG. 9. The variation of the major ion signals observed for the reaction of CH_3NH^- with CH_3Cl. T = 296 K, p = 0.465 torr, $\bar{v}$ = 9.6 × 10^3 cm s^{-1}, L = 60 cm, and the flow of CH_3NH_2 = 2.6 × 10^{18} molecule s^{-1}.

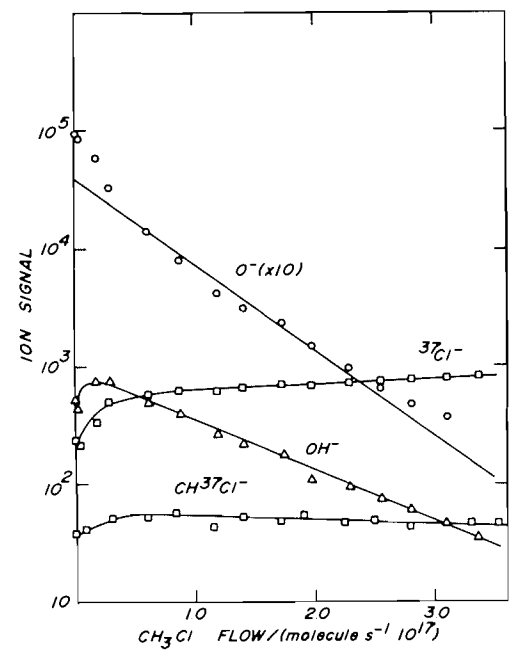

FIG. 10. The variation of the major ion signals observed for the reaction of O^- with CH_3Cl. T = 298 K, p = 0.397 torr, $\bar{v}$ = 8.2 × 10^3 cm s^{-1}, L = 60 cm, and the flow of air ~ 3 × 10^{17} molecule s^{-1}.

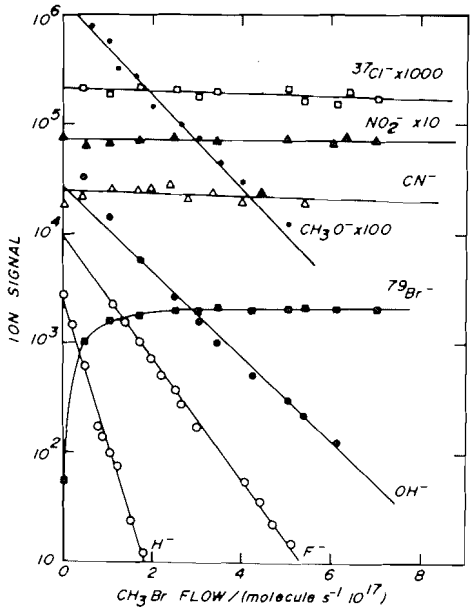

FIG. 11. Summary plot of the variation of anion signals observed as a function of CH_3Br flow. T = 298 K, p = 0.461 torr, $\bar{v} = 8.3 \times 10^3$ cm s^{-1}, L = 60 cm, and the flow of $H_2O \sim 5 \times 10^{17}$ molecule s^{-1} (OH^-, Cl^-, and NO_2^-), of $CH_3OH \sim 6 \times 10^{17}$ molecule s^{-1} (CH_3O^-), of $CF_4 = 1.4 \times 10^{17}$ molecule s^{-1} (F^-), and of $NH_3 = 1.3 \times 10^{18}$ molecule s^{-1} (H^- and CN^-).

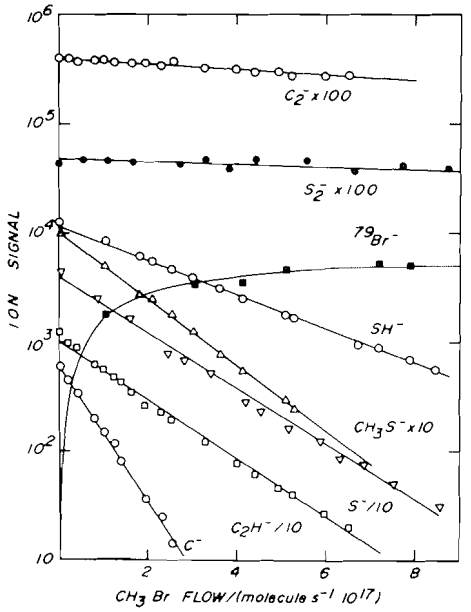

FIG. 12. Summary plot of the variation of anion signals observed as a function of CH_3Br flow. T = 295 K, p = 0.342 torr, $\bar{v} = 8.3 \times 10^3$ cm s^{-1}, L = 85 cm, and the flow of $C_2H_2 = 6.6 \times 10^{17}$ molecule s^{-1} (C^-, C_2^-, C_2H^-), of $CH_3SH = 4.3 \times 10^{17}$ molecule s^{-1} (S^-, SH^-, CH_3S^-) and of $CH_3SH = 2.3 \times 10^{18}$ molecule s^{-1} (S_2^-).

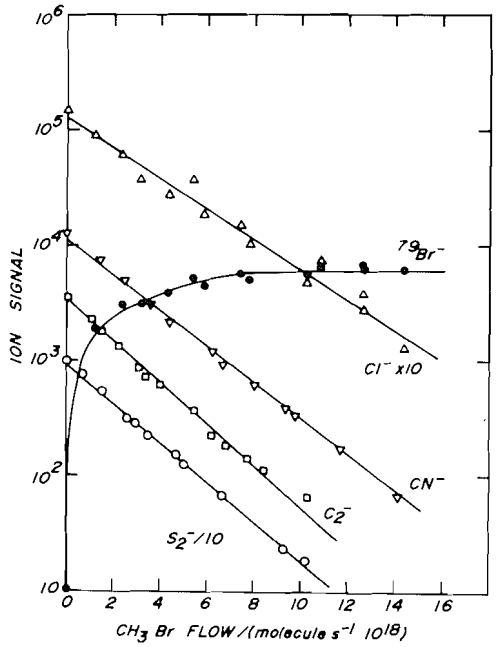

FIG. 13. Summary plot of the variation of anion signals observed as a function of CH_3Br flow. T = 296 K, p = 0.348 torr, $\bar{v} = 8.2 \times 10^3$ cm s^{-1}, L = 85 cm, and the flow of $C_2H_2 = 4.6 \times 10^{17}$ molecule s^{-1} (C_2^-), of $CH_3SH = 4.9 \times 10^{18}$ molecule s^{-1} (S_2^-), of $CH_3NH_2 = 2.4 \times 10^{18}$ molecule s^{-1} (CN^-), and of $CCl_4 \sim 5 \times 10^{17}$ molecule s^{-1} (Cl^-).

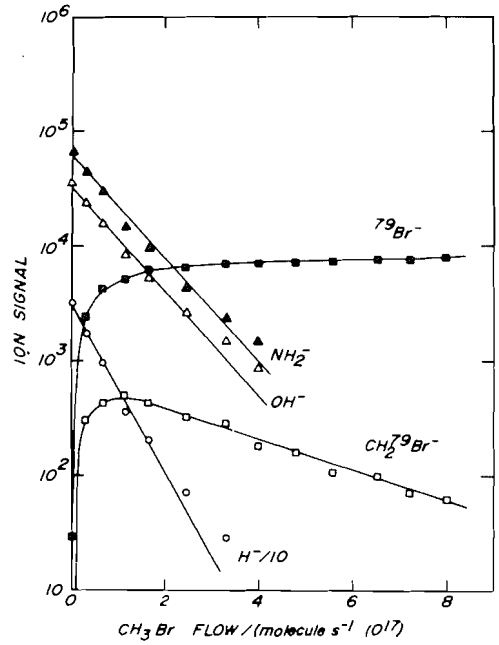

FIG. 14. The variation of the major ion signals observed for the reaction of NH_2^- with CH_3Br. T = 296 K, p = 0.531 torr, $\bar{v} = 9.5 \times 10^3$ cm s^{-1}, L = 61 cm, and the flow of $NH_3 = 3.9 \times 10^{18}$ molecule s^{-1}.

TABLE 4. Measured reaction and calculated capture rate constants (in units of 10^{-9} cm^3 molecule^{-1} s^{-1}) for exothermic reactions of anions with CH_3Br in the gas phase at 297 ± 2 K

Anion	N[a]	k_{expt} This work[b]	k_{expt} Other values	k_c[c]	k_{expt}/k_c[d]	$-\Delta H^0_{298}$/(kcal mol^{-1})
H^-	3	3.7±0.6		8.7	0.43±0.09	95±5
O^-	5	1.1±0.1		2.3	0.48±0.09	66±4
C^-	4	1.3±0.2		2.7	0.48±0.11	64±6
F^-	4	1.2±0.1	0.60±0.06 (5)	2.2	0.59±0.09	39±7
S^-	1	0.46		1.8	0.26±0.05	31±7
Cl^-	4	0.021±0.001	0.080±0.010 (5)	1.7	0.012±0.003	7±8
OH^-	4	0.99±0.09		2.3	0.43±0.09	57±6
C_2^-	3	0.032±0.002		2.0	0.016±0.003	44±36
CN^-	4	0.030±0.003		1.9	0.016±0.003	43±8[e]
SH^-	4	0.30±0.02		1.7	0.18±0.03	29±5
S_2^-	1	0.033		1.4	0.024±0.005	8±9
C_2H^-	3	0.52±0.05		1.9	0.26±0.07	73±25[f]
NH_2^-	5	1.1±0.1		2.3	0.48±0.09	71±6
NO_2^-	1	⩽0.001		1.6	⩽0.0006	14±6[g]
CH_2Br^-	3	0.42±0.03		1.3	0.32±0.06	
CH_3O^-	2	1.1±0.1		1.8	0.61±0.11	62±7
CH_3S^-	3	0.52±0.05	0.14±0.02 (5)	1.5	0.35±0.06	43±6
CH_3NH^-	3	1.3±0.1		1.8	0.72±0.14	82±9

[a] N is the number of measurements.
[b] The limits given along with the mean value of the measurements represent the best estimate of the precision (27). The accuracy is estimated to be ±20%.
[c] The capture rate constant is calculated using the Average-Dipole-Orientation Theory (28) with $C = 0.19$.
[d] The uncertainty in k_{expt}/k_c reflects only the accuracy of k_{expt}.
[e] For the formation of CH_3—CN.
[f] For the formation of CH_3—C≡CH.
[g] For the formation of CH_3—NO_2.

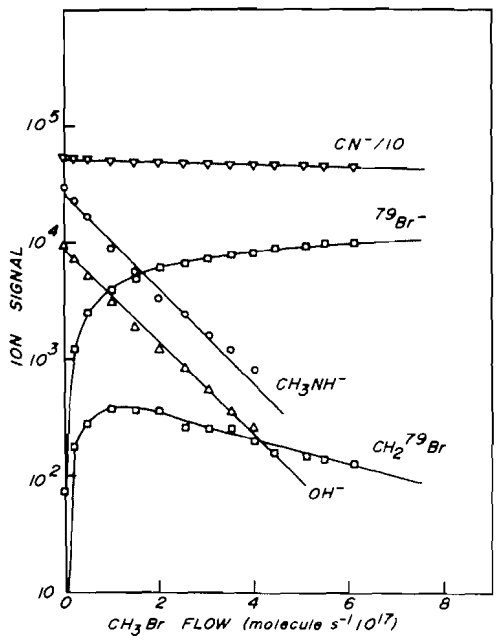

FIG. 15. The variation of the major ion signals observed for the reaction of CH_3NH^- with CH_3Br. $T = 296$ K, $p = 0.459$ torr, $\bar{v} = 9.7 \times 10^3$ cm s^{-1}, $L = 60$ cm, and the flow of $CH_3NH_2 = 1.7 \times 10^{18}$ molecule s^{-1}.

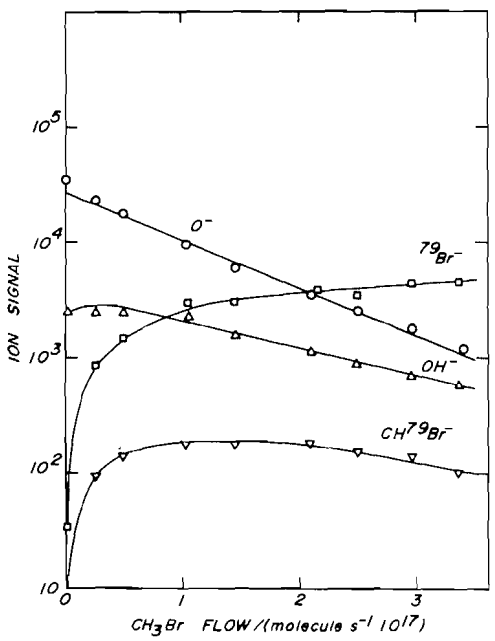

FIG. 16. The variation of the major ion signals observed for the reaction of O^- with CH_3Br. $T = 298$ K, $p = 0.404$ torr, $\bar{v} = 9.5 \times 10^3$ cm s^{-1}, $L = 60$ cm, and the flow of air $\sim 5 \times 10^{17}$ molecule s^{-1}.

all of which Br^- was the only observed product channel. A large range in the values of the rate constants for these reactions was again apparent.

The displacement reactions of NH_2^- and CH_3NH^- were again observed to compete with proton transfer as displayed in Figs. 14 and 15. The proton transfer product CH_2Br^- reacts further with CH_3Br according to

[9] $$CH_2Br^- + CH_3Br \rightarrow Br^- + (C_2H_5Br)$$

O^- was observed to react with CH_3Br as shown in Fig. 16 in a manner analogous to the CH_3Cl and CH_3F reactions

[10a] $$O^- + CH_3Br \rightarrow Br^- + CH_3O$$

[10b] $$\rightarrow OH^- + CH_2Br$$

[10c] $$\rightarrow CHBr^- + H_2O$$

The relative magnitude of the Br^- displacement channel is enhanced still further.

Discussion

The results summarized in Tables 2 to 4 revealed several kinetic features which can serve to characterize and classify the intrinsic reactivities of anions towards methyl halides.

(1) The specific rates of exothermic displacement reactions of anions with methyl halides are generally much higher in the gas phase than in solution.

As predicted by Moelwyn-Hughes and coworkers (2), many S_N2 reactions of type [1] do indeed proceed extremely rapidly in the gas phase especially the reactions with CH_3Cl and CH_3Br. The reactions with CH_3F are generally at least ~ 100 times slower. Table 5 provides a comparison of bimolecular specific rates for several displacement reactions investigated in both the gas phase and solution. It is readily apparent that the specific rates in the gas phase exceed those in solution by many orders of magnitude, *viz.* by factors of $\gtrsim 10^{10}$. This disparity in the magnitude of the specific rates must reflect the effect of solvent on intrinsic reactivity so that one would expect a lowering in the specific rate in the gas phase as a result of the selective solvation of the 'nude' nucleophile by one or more solvent molecules. Such a lowering in specific rate has been observed previously for displacement reactions of 'nude' and solvated alkoxide ions with CH_3Cl (3).

In the gas phase the specific rate of the displacement reactions of type [1] is limited by the

TABLE 5. A comparison of bimolecular specific rates and apparent activation energies for several displacement reactions investigated *in vacuo* and in solution

Reactants $CH_3Y + X^-$	Solution			Gas phase	
	Solvent	$k_{298\,K}$ (cm^3 $molecule^{-1}$ s^{-1})	E_a (kcal mol^{-1})	$k_{297\,K}$ cm^3 $molecule^{-1}$ s^{-1}	E_a[a] (kcal mol^{-1})
$CH_3F + OH^-$	H_2O[b]	9.7×10^{-28}	21.6	$(2.5\pm0.5)\times10^{-11}$	2.7 ± 0.1
$CH_3Cl + OH^-$	H_2O[b]	1.0×10^{-26}	24.3	$(1.5\pm0.3)\times10^{-9}$	0.28 ± 0.14
$CH_3Cl + F^-$	H_2O[b]	2.5×10^{-29}	26.9	$(1.8\pm0.4)\times10^{-9}$	0.15 ± 0.13
$CH_3Br + OH^-$	H_2O[b]	2.3×10^{-25}	23.0	$(9.9\pm2.0)\times10^{-10}$	0.50 ± 0.14
$CH_3Br + F^-$	H_2O[b]	5.6×10^{-28}	25.2	$(1.2\pm0.2)\times10^{-9}$	0.31 ± 0.14
$CH_3Br + Cl^-$	H_2O[b]	8.2×10^{-27}	24.7	$(2.1\pm0.4)\times10^{-11}$	2.6 ± 0.1
	CH_3OH[c]	1.1×10^{-26}			
	DMF[d]	6.7×10^{-22}			
	MeCO[d]	5.3×10^{-21}			

[a]The uncertainty in E_a reflects only the uncertainty in the measured specific rate, 297 K.
[b]Reference 2.
[c]Reference 40.
[d]Reference 1.

collision or capture rate just as the diffusion rate provides an upper limit in solution. The capture rate is readily estimated from current classical theories of collision. For collisions between ions and neutral polar substrates having a Maxwell–Boltzmann energy distribution, the Average-Dipole-Orientation (ADO) theory of Su and Bowers (28) has proven to predict the capture rate at 297 K most adequately (29, 30). According to this theory the capture rate constant is given by

$$[11]\quad k_c = 2\pi e\left(\frac{\alpha}{\mu}\right)^{1/2} + C\left(\frac{2\pi e\mu_D}{\mu}\right)\left(\frac{2\mu}{\pi kT}\right)^{1/2}$$

where e is the charge on the ion, μ the reduced mass of the collidants, α the polarizability and μ_D the permanent dipole moment of the molecule. C is the 'dipole locking' constant which can be determined from the polarizability and permanent dipole moment of the neutral substrate (28). Tables 2, 3, and 4 include values of k_c calculated for all the reactions investigated in this study. Values for μ_D and α were taken from Rothe and Bernstein (31). The ratio $(k_{exptl}/k_c)_{297\,K}$ is a measure of the reaction probability per collision. An inspection of the values of k_{exptl}/k_c provided in Tables 2, 3, and 4 indicates that whereas many of the reactions proceed essentially upon every collision, a large group of exothermic reactions proceed on at most every 100 collisions.

(2) Many exothermic displacement reactions of anions with methyl halides apparently have activation energies in the gas phase.

Displacement reactions are characterized in solution by large activation energies, $E_a \sim 15$–30 kcal mol^{-1} (see Table 5). These activation energies are usually associated with the work required to break down initial state solvation. Nevertheless, some concern has been expressed regarding the extent to which these observed activation energies reflect intrinsic properties of the reacting systems. Parker has drawn attention to the caution which should be exercised in any attempt to extract such information from solution measurements of specific rates (1). Quantum mechanical calculations of portions of the intrinsic energy surfaces of displacement reactions of type [1] have in fact indicated the presence of what are, in some instances, quite substantial energy barriers (8, 9). The gas-phase (single temperature) measurements reported here can also provide some indication of the possible presence and magnitude of these intrinsic activation energies.

The magnitude of the activation energy can be estimated from the reaction probability per collision, k_{exptl}/k_c, in the traditional Arrhenius manner if the following expression is assumed to be approximately valid (32)

$$[12]\quad k_{exptl} = k_c \exp(-E_a/RT)$$

Although such a treatment is a gross oversimplification in that it completely ignores constraints to reaction resulting from short-range interactions, *e.g.* orientation or steric effects, there is some evidence (7) that it is reasonable to a first approximation for displacement re-

TABLE 6. Apparent activation energies[a] (in kcal mol^{-1}) for exothermic displacement reactions with CH_3F, CH_3Cl, and CH_3Br *in vacuo*

Nucleophile	CH_3F	CH_3Cl	CH_3Br
H^-	3.7 ± 0.1	0.62 ± 0.73	0.50 ± 0.14
C^-	$\geqslant 4.2$	1.3 ± 0.1	0.43 ± 0.16
F^-		0.1 ± 0.1	0.31 ± 0.10
S^-		2.4 ± 0.2	0.80 ± 0.10
Cl^-			2.6 ± 0.2
OH^-	2.7 ± 0.2	0.28 ± 0.14	0.50 ± 0.14
C_2^-	$\underline{\geqslant 4.1}$	$\geqslant 3.8$	2.5 ± 0.1
CN^-	$\underline{\geqslant 3.8}$	$\geqslant 5.0$	2.4 ± 0.2
SH^-		2.8 ± 0.1	1.0 ± 0.1
S_2^-		$\underline{\geqslant 4.4}$	2.2 ± 0.1
C_2H^-	$\geqslant 4.5$	1.6 ± 0.2	0.80 ± 0.18
NH_2^-	2.9 ± 0.1	0.3 ± 0.1	0.43 ± 0.13
NO_2^-		$\underline{\geqslant 4.4}$	$\geqslant 4.4$
CH_3O^-	2.9 ± 0.1	$\underline{0.23}\pm0.13$	0.29 ± 0.12
CH_3S^-	$\underline{\geqslant 4.3}$	1.6 ± 0.1	0.62 ± 0.11
CH_3NH^-	$\underline{2.1}\pm0.2$	0.1 ± 0.1	0.19 ± 0.13

[a]Values underlined correspond to reactions which, within the uncertainty of ΔH^0_{298}, may in fact be endothermic by an amount $\gtrsim$ the calculated value for E_a.

actions of type [1]. Nevertheless we recognize that this approach is somewhat speculative and perhaps too enterprising but feel that it is warranted at this stage of development of our knowledge of activation energies in ion–molecule reactions. Clearly the activation energies determined in this manner should be viewed with caution until rate measurements at several temperatures become available. Table 6 summarizes the magnitudes of the apparent activation energies determined using eq. 12. The values range from $\sim 0-\gtrsim 5$ kcal mol^{-1} and a definite trend in reactivity can be identified. The nucleophiles H^-, F^-, OH^-, CH_3O^-, NH_2^-, and CH_3NH^- appear to react with CH_3Cl and CH_3Br with little or no activation energy ($E_a < 1$ kcal mol^{-1}) whereas their corresponding reactions with CH_3F (excluding $F^- + CH_3F$) exhibit apparent activation energies $2 < E_a < 4$ kcal mol^{-1}. The reactions of the remaining nucleophiles exhibit a similar decrease in apparent activation energy in going from CH_3F to CH_3Cl to CH_3Br with the reactivities of C_2^-, S_2^-, CN^-, and Cl^- remaining low ($E_a > 2$ kcal mol^{-1}) even with CH_3Br.

(3) The nucleophiles may be conveniently classified according to their reactivity and its variation with heat of reaction.

In an attempt to correlate the magnitudes of the apparent activation energies with some simple property of the reacting systems, we have found most useful the empirical expression established about 40 years ago by Evans and Polanyi (33) which relates the activation energy of a reaction to its heat of reaction according to

$$E_a = \alpha\Delta H + C \qquad [13]$$

where $0 < \alpha < 1$ and C is a constant for a homologous series. Expression [13] can be arrived at qualitatively from a consideration of the attractive and repulsive potential energy curves for a series of homologous reactions of varying exothermicity (33, 34). The applicability of the Polanyi relation has been clearly established for a few series of neutral reactions of very closely related compounds (34). However, experimental results for gas-phase ion–molecule reactions which often have no apparent activation energy have not been subjected to such a correlation. M. Polanyi and co-workers did, however, include negative-ion displacement reactions of type [1] amongst the reactions for which relation [13] was developed and in fact attempted to predict activation energies for such reactions proceeding in solution at a time when gas-phase results were unavailable (35).

The Polanyi relation predicts an activation energy which approaches the heat of reaction for highly endothermic processes and becomes negative for sufficiently exothermic reactions. Johnston has developed an analogous empirical expression which constrains the activation energy to approach zero for highly exothermic reactions (36).

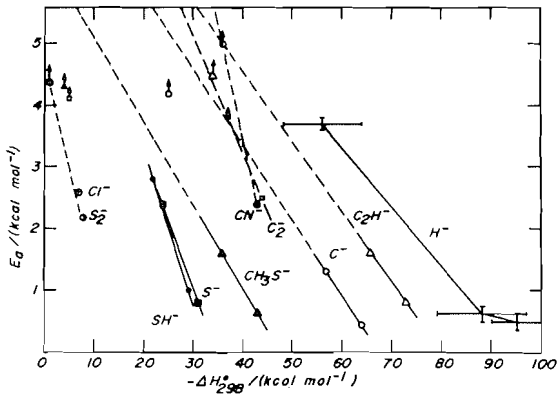

FIG. 17. A plot of the apparent activation energy *vs.* reaction exothermicity for a series of homologous reactions of specific anions with CH_3F, CH_3Cl, and CH_3Br. The uncertainties in E_a and ΔH^0_{298} displayed for the H^- series is approximately representative of the uncertainties associated with the other anion series. The plots for each anion series (excluding the H^- series) assume a linear relationship between E_a and ΔH^0_{298}.

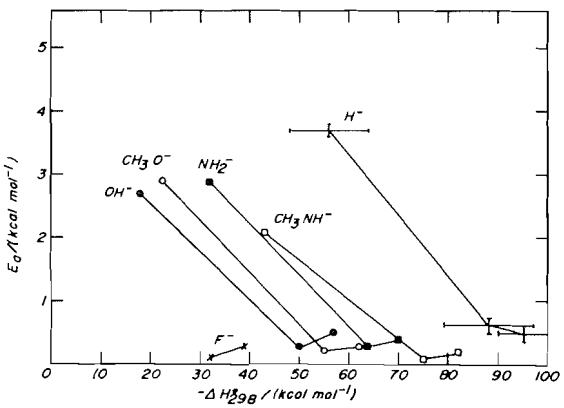

FIG. 18. A plot of the apparent activation energy *vs.* reaction exothermicity for series of homologous reactions of CH_3F, CH_3Cl, and CH_3Br with F^-, OH^-, CH_3O^-, NH_2^-, CH_3NH^-, and H^-, respectively. The uncertainties in E_a and ΔH^0_{298} displayed for the H^- series is approximately representative of the uncertainties associated with the other anion series.

A number of series of homologous reactions can be identified from the reactions investigated in this study. Consider, for example, the homologous series of reactions between a specific anion A^- and the three methyl halides, *viz.*

$$[14] \qquad A^- + CH_3Y \rightarrow CH_3A + Y^-$$

where Y = F, Cl, or Br. For such series of reactions, the exothermicity increases from CH_3F to CH_3Br in accordance with the decrease

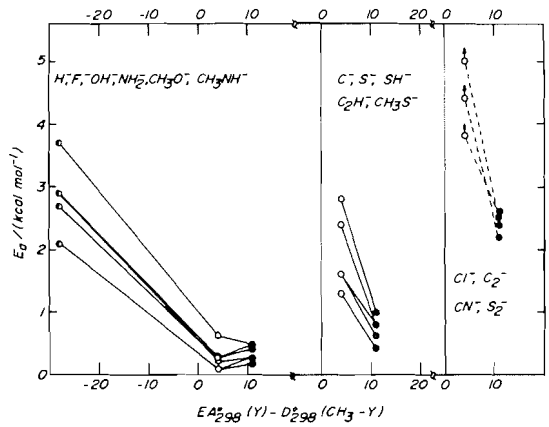

FIG. 19. A classification of nucleophiles according to their Polanyi–Johnston characteristics for series of homologous displacement reactions with CH_3F(◐), CH_3Cl(○) and CH_3Br(●).

in the intrinsic thermodynamic nucleophilicity of the halogen, *viz.* F > Cl > Br, which is largely determined by $D(CH_3—Y)$ since the electron affinities of F, Cl, and Br are very nearly equal. Figures 17 and 18 explore the variations of the apparent activation energies in Table 6 for such series of reactions with exothermicity. The variations generally fit a pattern remarkably consistent with the Polanyi–Johnston expressions which in turn enhances our confidence in the reality of the presence of activation energies in the displacement reactions under study. Those reactions in a homologous series in which a strong bond is broken are generally less probable than those in which the bond is weak. The variations for the S_2^-, SH^-, S^-, CH_3S^-, CN^-, C_2^-, C^-, and C_2H^- series can be fit with the Polanyi relation with values of α in the range 0.1 to 0.3. The variations for the F^-, OH^-, CH_3O^-, NH_2^-, CH_3NH^-, and H^- series are more consistent with an empirical expression of the type derived by Johnston since the apparent activation energies approach zero for the more exothermic reactions with CH_3Cl and CH_3Br. Also one expects, and indeed can observe, a similar accord with the Polanyi–Johnston relations for groups of homologous reactions of a specific halide with a series of homologous anions, *e.g.* S^-, SH^-, CH_3S^-, and S_2^- or NH_2^- and CH_3NH^- or OH^- and CH_3O^-.

A consideration of the magnitudes of the apparent activation energies and their variation

TABLE 7. Predicted values for the apparent activation energies (in kcal mol^{-1}) of exothermic and thermoneutral displacement reactions with CH_3F and CH_3Cl in the gas phase

$X^- + CH_3Y$	E_a	Other results	$-\Delta H^0_{298}$ (kcal mol^{-1})
$C^- + CH_3F$	5.2		25 ± 10
$F^- + CH_3F$	~3	7.9 (8)[a]	0
$C_2^- + CH_3F$	$\gtrsim 10$		7 ± 37
$CN^- + CH_3F$	$\gtrsim 17$	22 (9)[a]	4 ± 11
$C_2H^- + CH_3F$	5.2		34 ± 28
$Cl^- + CH_3Cl$	$\gtrsim 4.5$	~3.4 (5)[b]	0

[a]Computed heights of energy barriers.
[b]Apparent activation energy deduced from a measured rate constant $k_{298} \sim 6 \times 10^{-12}$ cm^3 $molecule^{-1}$ s^{-1}.

with exothermicity encountered in Figs. 17 and 18 suggests a convenient classification of the nucleophiles into three distinct groups according to Fig. 19 in which the apparent activation energies are plotted against the thermodynamic nucleophilicity of the halogen leaving group.

(*a*) Anions demonstrating high nucleophilicity: H^-, F^-, OH^-, NH_2^-, CH_3O^-, and CH_3NH^-. These anions all demonstrate high reactivity towards CH_3Cl and CH_3Br ($E_a < 1$ kcal mol^{-1}) and low reactivity towards CH_3F ($E_a > 2$ kcal mol^{-1}). Their Polanyi–Johnston characteristics are all of similar shape with α being dependent on exothermicity.

(*b*) Anions demonstrating medium nucleophilicity: C^-, S^-, SH^-, CH_3S^-, and C_2H^-. These anions are distinctly less reactive towards CH_3Cl ($E_a \gtrsim 2$ kcal mol^{-1}) than CH_3Br ($E_a \lesssim 1$ kcal mol^{-1}). Their reactions with CH_3F, when exothermic, appear to have activation energies $\gg 4$ kcal mol^{-1}. α has values in the range 0.1–0.3.

(*c*) Anions demonstrating low nucleophilicity: Cl^-, CN^-, C_2^-, and S_2^-. These anions are distinctly less reactive than the group *b* anions towards CH_3Br ($E_a > 2$ kcal mol^{-1}), CH_3Cl ($E_a > 3$ kcal mol^{-1}), and presumably also CH_3F ($E_a \gg 4$ kcal mol^{-1}). α has values $\gtrsim 0.2$. In each of the three groups the order of leaving group ability (LGA) is $Br^- \gtrsim Cl^- > F^-$.

The empirical correlations established for the three groups of anions allow predictions of values for the apparent activation energies of exothermic and thermoneutral displacement reactions not directly measurable in these experiments. These are summarized in Table 7. For the reactions of F^- and CN^- with CH_3F comparisons can be with the barrier heights computed by Dedieu and Veillard (8) and Bader *et al.* (9). Within the uncertainty of the empirical correlation and its extrapolation the accord between theory and experiment is reasonable. Brauman *et al.* (5) have reported a measured rate constant for the displacement reaction of Cl^- with CH_3Cl which can be reduced to an apparent activation energy $E_a \sim 3.4$ kcal mol^{-1}, in fair agreement with the extrapolated value of $E_a \gtrsim 4.5$ kcal mol^{-1}.

(4) Displacement in the gas phase at 298 K may proceed in competition with other reaction channels.

A variety of channels were observed for the reactions of several anions with methyl halides, *viz.* methyl cation transfer or S_N2, [1*a*], proton transfer, [1*b*], hydrogen atom transfer, [1*c*], and H_2^+ transfer, [1*d*]

$$[1a] \quad X^- + CH_3Y \rightarrow Y^- + CH_3X$$

$$[1b] \quad \rightarrow CH_2Y^- + XH$$

$$[1c] \quad \rightarrow XH^- + CH_2Y$$

$$[1d] \quad \rightarrow CHY^- + H_2X$$

Channel 1*b* becomes exothermic when $PA(X^-) > PA(CH_2Y^-)$, *i.e.* when the intrinsic Brønsted basicity of X^- exceeds that of CH_2Y^-. When the nucleophile, X^-, is a radical anion, the channels 1*c* and 1*d* become viable alternate channels since XH^- and H_2X are now likely to have a significant stability. Channel 1*c* becomes exothermic when the hydrogen-atom affinity of the nucleophile, *viz.* $D(X^-—H)$, exceeds the $H_2YC—H$ bond strength, *i.e.* when

$$[15] \quad D(XH) - EA(XH) + EA(X) > D(H_2YC—H)$$

Channel 1*d* becomes exothermic when

$$[16]\quad \Delta H^0_f(X^-) - \Delta H^0_f(H_2X) > \Delta H^0_f(CHY^-) - \Delta H^0_f(CH_3Y)$$

The intrinsic basicity order of the nucleophiles investigated in this study is as follows: $CH_3NH^- > NH_2^- > H^- > OH^- > CH_3O^- > C_2H^- > O^- > F^- > C^- > CH_3S^- > SH^- > CN^- > S^- > NO_2^- > Cl^- > Br^-$.[3] The basicities of C_2^- and S_2^- are not well established but are not likely to be very high. Competing proton transfer channels were observed only for the reactions of CH_3NH^- and NH_2^- with CH_3Cl and CH_3Br. These proton transfer channels are the most exothermic. It appears, therefore, that proton transfer will compete with displacement only if the nucleophile is also a strong base. The possibility remains however that proton transfer will compete only if it is exothermic in accordance with the basicity order $CH_2F^- > CH_3NH^- > NH_2^- > CH_2Cl^-, CH_2Br^- > H^-$. The intrinsic Brønsted acidities of CH_3F, CH_3Cl, and CH_3Br have not been determined previously.

Thermodynamic considerations indicate that, of the radical anions O^-, C^-, S^-, C_2^-, and S_2^-, only O^- is likely to have an H-atom affinity higher than the H_2YC—H bond strength which would explain why H-atom abstraction was observed only for the reactions of this anion. The H_2^+ transfer channel 1*d* is also the most exothermic for the reaction of O^- and was observed only with this anion.

Channels 1*a*, 1*c*, and 1*d* have been previously observed for the reactions of O^- with CH_3Cl by Bohme and Young (3) in a flowing afterglow (FA) experiment and for the reactions of CH_3F (channels 1*c* and 1*d* only), CH_3Cl and CH_3Br by Tiernan and Hughes[4] in a tandem mass spectrometer (tms) experiment at impacting ion energies of 0.3 ± 0.3 eV. The hydrogen atom transfer channel dominates in the reaction of O^- with CH_3F but decreases in importance in the reactions of O^- with CH_3Cl and CH_3Br. It may be of interest to note here that the reaction of O^- with CH_4, a possible fourth member in the homologous series of O^- reactions, has been observed to proceed only by hydrogen atom transfer (39).[4] Both the tms and FA experiments indicate an increasing contribution of the displacement channel to the overall reactions of O^- in progressing from CH_3F to CH_3Br. However, at the higher ion energies of the tms experiments H-atom transfer remains the dominant channel even for the reaction of O^- with CH_3Br. The branching ratio therefore appears to be sensitive to the initial energetics of the reacting system. A measure of the change in branching ratio with ion energy or temperature of the reacting system would no doubt be most instructive in providing further insight into the mechanisms of reactions of this type.

[3]The basicities of $X^- = H^-$, OH^-, O^-, F^-, C^-, SH^-, S^-, Cl^-, and Br^- were computed from known values for IP(H), EA(X) and $D^0_{298}(XH)$ as determined from $\Delta H^0_{f,298}$ (H, X, and XH) see refs. 11, 12, 14, 19, and 37. Measurements from this laboratory have provided values for the basicities of CH_3NH^- (25), NH_2^- (23), C_2H^- (22), and CN^- (38), and the relative basicities of CH_3O^- and CH_3S^-, unpublished results.

[4]T. O. Tiernan and B. M. Hughes, private communication.

Acknowledgments

The financial support of the National Research Council of Canada and the Sloan Foundation is gratefully acknowledged.

1. A. J. Parker. Chem. Rev. **69**, 1 (1969).
2. R. H. Bathgate and E. A. Moelwyn-Hughes. J. Chem. Soc. 2642 (1959).
3. D. K. Bohme and L. B. Young. J. Am. Chem. Soc. **92**, 7354 (1970).
4. L. B. Young, E. Lee-Ruff, and D. K. Bohme. J. Chem. Soc. Chem. Commun. 35 (1973).
5. J. I. Brauman, W. N. Olmstead, and C. A. Lieder. J. Am. Chem. Soc. **96**, 4030 (1974).
6. C. M. Won and A. V. Willi. J. Phys. Chem. **76**, 427 (1972).
7. D. K. Bohme, G. I. Mackay, and J. D. Payzant. J. Am. Chem. Soc. **96**, 4027 (1974).
8. A. Dedieu and A. Veillard. J. Am. Chem. Soc. **94**, 6730 (1972).
9. R. F. Bader, A. J. Duke, and R. R. Messer. J. Am. Chem. Soc. **95**, 7715 (1973).
10. D. K. Bohme, R. S. Hemsworth, H. W. Rundle, and H. I. Schiff. J. Chem. Phys. **58**, 3504 (1973).
11. JANAF thermochemical tables. 2nd ed. Natl. Stand. Ref. Data Ser. Natl. Bur. Stand. **37** (1971).
12. B. deB. Darwent. Natl. Stand. Ref. Data Ser. Natl. Bur. Stand. **31**, (1970).
13. S. W. Benson. Thermochemical kinetics. John Wiley and Sons, Inc., New York, N.Y. 1968.
14. JANAF thermochemical tables. 1974 Suppl. J. Phys. Chem. Ref. Data, **3**, 311 (1974).
15. W. C. Lineberger and B. W. Woodward. Phys. Rev. Lett. **25**, 424 (1970).

16. J. L. FRANKLIN, J. G. DILLARD, H. M. ROSENSTOCK, J. T. HERRON, K. DRAXL, and F. H. FIELD. Ionization potentials, appearance potentials and heats of formation of gaseous positive ions. Natl. Stand. Ref. Data Ser. Natl. Bur. Stand. **26** (1969).
17. R. S. BERRY and C. W. REIMANN. J. Chem. Phys. **38**, 1540 (1963).
18. V. H. DIBELER and S. K. LISTON. J. Chem. Phys. **49**, 482 (1968).
19. L. M. BRANSCOMB. Phys. Rev. **148**, 11 (1966).
20. R. J. CELOTTA, R. A. BENNET, and J. L. HALL. J. Chem. Phys. **60**, 1740 (1974).
21. H. OKABE and V. H. DIBELER. J. Chem. Phys. **59**, 2430 (1973).
22. D. K. BOHME, G. I. MACKAY, H. I. SCHIFF, and R. S. HEMSWORTH. J. Chem. Phys. **61**, 2175 (1974).
23. D. K. BOHME, R. S. HEMSWORTH, and H. W. RUNDLE. J. Chem. Phys. **59**, 77 (1973).
24. D. K. SEN SHARMA and J. L. FRANKLIN. J. Am. Chem. Soc. **95**, 6562 (1973).
25. G. I. MACKAY, R. S. HEMSWORTH, and D. K. BOHME. Can. J. Chem. This issue.
26. K. W. EGGER and A. T. COCKS. Helv. Chim. Acta, **56**, 1516 (1973).
27. N. C. BARFORD. Experimental measurements: precision, error and truth. Addison-Wesley, London. 1967.
28. T. SU and M. T. BOWERS. Int. J. Mass Spectrom. Ion Phys. **12**, 347 (1973).
29. M. T. BOWERS and T. SU. Theory of ion – polar molecule collisions. *In* Interactions between ions and molecules. *Edited by* P. Ausloos. Plenum Press, New York. 1975.
30. D. K. BOHME. The kinetics and energetics of proton transfer. *In* Interactions between ions and molecules. *Edited by* P. Ausloos. Plenum Press, New York. 1975.
31. E. W. ROTHE and R. B. BERNSTEIN. J. Chem. Phys. **31**, 1619 (1959).
32. H. I. SCHIFF and D. K. BOHME. Int. J. Mass Spectrom. Ion Phys. **16**, 167 (1975).
33. M. G. EVANS and M. POLANYI. Trans. Faraday Soc. **34**, 11 (1938).
34. N. N. SEMENOV. Some problems in chemical kinetics and reactivity. Vol. 1. (translated by M. Bondart). Princeton University Press, Princeton, N.J. 1958.
35. R. A. OGG and M. POLANYI. Trans. Faraday Soc. **31**, 604 (1935).
36. H. S. JOHNSTON. Gas phase reaction rate theory. The Ronald Press Company, New York. 1966.
37. H. HOTOP and W. C. LINEBERGER. J. Phys. Chem. Ref. Data. In press.
38. D. BETOWSKI, G. MACKAY, J. PAYZANT, and D. BOHME. Can. J. Chem. **53**, 2365 (1975).
39. D. K. BOHME and F. C. FEHSENFELD. Can. J. Chem. **47**, 2717 (1969).
40. R. ALEXANDER, E. C. F. KO, A. J. PARKER, and T. J. BROXTON. J. Am. Chem. Soc. **90**, 5049 (1968).